MITSUBISHI ELECTRIC RESEARCH LABORATORIES
http://www.merl.com

Modeling Cutting Forces for 5-Axis Machining of Sculptured Surfaces

Boz, Y.; Erdim, H.; Lazoglu, I.

TR2011-043 May 2011

Abstract

5-axis ball-end milling processes are used in various industries such as aerospace, automotive, die-mold and biomedical industries. 5-axis machining provides reduced cycle times and more accurate machining via reduction in machining setups, use of shorter tools due to improved tool accessibility. However, desired machining productivity and precision can be obtained by physical modeling of machining processes via appropriate selection of process parameters. In response to this gap in the industry this paper presents a cutting force model for 5-axis ball-end milling cutting force prediction. Cutter-workpiece engagement is extracted via developed solid modeler based engagement model. Simultaneous 5-axis milling tests are conducted on Al7075 workpiece material with a carbide cutting tool. Validation of the proposed model is performed for impeller hub roughing tool paths. Validation test proves that presented model is computationally efficient and cutting forces can be predicted reasonably well. The result of validation test and detailed comparison with the simulation are also presented in the paper.

CIRP Conference on Modelling of Machining Operations

Advanced Materials Research Vol. 223 (2011) pp 701-712

doi:10.4028/www.scientific.net/AMR.223.701

Modeling Cutting Forces for Five Axis Milling of Sculptured Surfaces

Y. Boz [1], H. Erdim [2], I. Lazoglu [1*]

[1] Manufacturing and Automation Research Center, Koc University, Turkey
[2] Mitsubishi Electric Research Laboratories, USA
[*] ilazoglu@ku.edu.tr

Keywords: Free form surface, 5 axis, machining, milling, force, kinematic, mechanics

Abstract. 5-axis ball-end milling processes are used in various industries such as aerospace, automotive, die-mold and biomedical industries. 5-axis machining provides reduced cycle times and more accurate machining via reduction in machining setups, use of shorter tools due to improved tool accessibility. However, desired machining productivity and precision can be obtained by physical modeling of machining processes via appropriate selection of process parameters. In response to this gap in the industry this paper presents a cutting force model for 5-axis ball-end milling cutting force prediction. Cutter-workpiece engagement is extracted via developed solid modeler based engagement model. Simultaneous 5-axis milling tests are conducted on Al7075 workpiece material with a carbide cutting tool. Validation of the proposed model is performed for impeller hub roughing toolpaths. Validation test proves that presented model is computationally efficient and cutting forces can be predicted reasonably well. The result of validation test and detailed comparison with the simulation are also presented in the paper.

Introduction

5-axis machining technologies are used in the production of various parts in aerospace, die-mold, automotive and biomedical industries. With 5-axis machining, complex shapes can be machined in a single setup which reduces cycle times. Improved tool accessibility allows the use of shorter tools that provide more accurate machining. The main aims of using 5-axis machining in industry are to reduce cycle times, dimensional and surface errors in its nature. However, this cannot be achieved satisfactorily without the physical modeling of the milling process. Furthermore, while machining free-form surfaces local peak forces may occur due to spatially changing engagement between the cutter and the workpiece. Hence, cutting force modeling gains more importance in order to prevent excessive cutter deflection and surface errors in these processes.

Most of the research on 5- axis machining focused on the geometric aspects of this process such as toolpath generation, toolpath optimization and geometric verification of the toolpath. With the improvement in the CAM technology geometric constraints and errors can be eliminated, on the other hand, the physics of the process is not considered. Consequently, efficiency of the process and errors due to physical constraints cannot be predicted before the production of the part.

Fussell et al. [1] developed a 5-axis virtual machining environment for discrete simulation of sculptured surface machining which aims automatic feedrate selection along the toolpath via mechanistic modeling of cutting forces. Bailey et al. 2] proposed a generic mechanistic cutting force model for simulating multi axis machining of sculptured surfaces. A process optimization tool was presented by employing a feedrate scheduling method using the maximum chip load and cutting force as constraints.

One of the most recent studies on modeling of 5- axis milling was carried out by Ozturk and Budak [3]. Analytical modeling of cut geometry of 5-axis machining was performed and obtained data was used for cutting force prediction and process optimization. Ferry and Altintas [4] developed a virtual machining simulation system for 5-axis flank milling of jet engine impellers.

This article extends the modeling of 3-axis ball-end milling presented by Erdim et al. [5, 6] into mechanistic modeling of 5-axis ball-end milling. Boundary representation (B-rep) based exact Boolean method is preferred for extracting cutter-workpiece engagement due to its efficiency and speed over other discrete methods. Developed engagement model can easily handle complex engagements between tool and workpiece. Comprehensive formulation of the cutting force model and its validation with 5-axis machining tests are presented. Cutting force predictions are shown to be in good agreement with experiments.

Kinematics of 5-Axis Milling

5-axis milling geometry differs from 3-axis milling geometry. In 3-axis milling, tool movement is given as three translational motions along the X-Y-Z coordinate frame axes. In 5-axis milling, two additional rotary axes are present. Consequently, tool motion is defined as a combination of three translational motions and two rotational motions.
Rotational motion in 5-axis milling is represented by lead and tilt angles. Lead angle is defined as the rotation angle about $\boldsymbol{Y}_w$ which is Y axis of workpiece coordinate frame. Tilt angle is the rotation angle about $\boldsymbol{X}_w$ which is the X axis of the workpiece coordinate frame. Definition of the lead and tilt angles and the illustration of the coordinate frames are shown in Figure 1 where $(\boldsymbol{X}_f - \boldsymbol{Y}_f - \boldsymbol{Z}_f)$ is the feed coordinate frame.

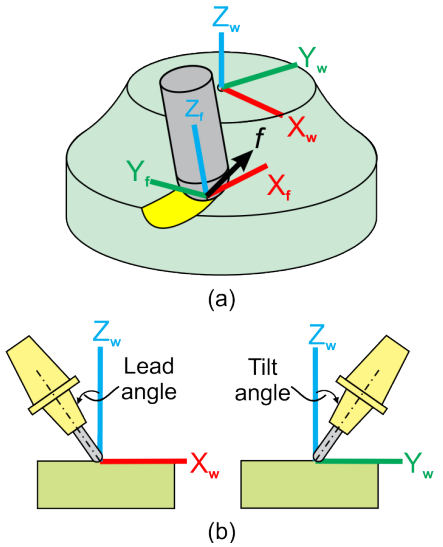

Figure 1: (a) Illustration of coordinate frames; (b) lead and tilt angles.

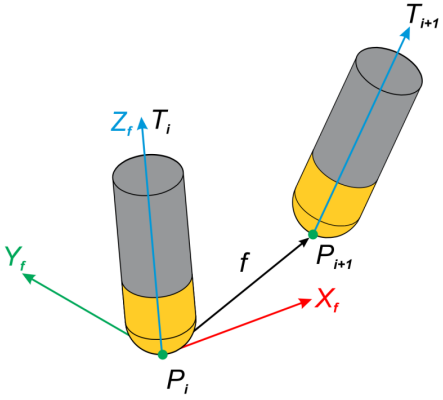

Figure 2: Feed vector and feed coordinate frame.

Feed vector $\boldsymbol{f}$ can be expressed as,

$$\boldsymbol{f} = (\boldsymbol{P}_{i+1} - \boldsymbol{P}_i)/\|\boldsymbol{P}_{i+1} - \boldsymbol{P}_i\| \quad (1)$$

Another important property regarding feed coordinate frame is that, the feed direction and the cross feed direction denoted as $\boldsymbol{X}_f$ and $\boldsymbol{Y}_f$ respectively have to lie in a plane where the normal of this plane is $\boldsymbol{T}_i$. In other words, an orthogonal basis is defined using tool axis vector $\boldsymbol{T}_i$ and feed vector $\boldsymbol{f}$ where Z axis of the feed coordinate frame $\boldsymbol{Z}_f$ is coincident with the tool axis orientation $\boldsymbol{T}_i$ at cutter location i.

$$\boldsymbol{Y}_f = \boldsymbol{T}_i \times \boldsymbol{f} \tag{2}$$

$$\boldsymbol{X}_f = \boldsymbol{Y}_f \times \boldsymbol{T}_i \tag{3}$$

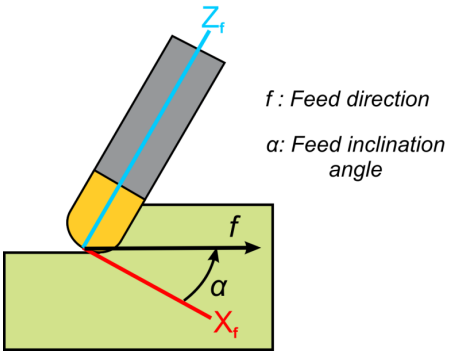

Figure 3: Illustration of feed inclination

Due to 5-axis tool motion, feed inclination angle α is calculated with respect to horizontal feed direction $\boldsymbol{X}_f$ as shown in Figure 3,

$$\alpha = atan2(\boldsymbol{f} \cdot \boldsymbol{Z}_f, \boldsymbol{f} \cdot \boldsymbol{X}_f) \tag{4}$$

where $atan2$ is a four-quadrant arctangent function.

Cutter-workpiece engagement model

In sculpture surface machining, the cutter-workpiece engagement region does vary along the cutter path and in general, unless some specific and very simple workpiece geometry is machined, it is difficult to find an exact analytical representation for the engagement region. Chip load and force calculations are based on the cutter-workpiece engagements; therefore the output of the engagement model is very critical. Mathematically, the swept volume is the set of all points in space encompassed within the object envelope during its motion. The mathematical formulation of the swept volume computation has been investigated using singularity theory, envelope theory, jacobian rank deficiency method, sweep differential equation (SDE), minkowski sums, implicit modeling and kinematics.

The basic idea is mathematically removing the swept volume generated by cutter movements along the NC trajectory (3 or 5-axis motions) from the model of the raw stock, and thus obtaining in-process or final machined workpiece. From the literature, the NC simulation methods can be categorized into three major approaches; Solid modeling, spatial partitioning and discrete vectors. The direct Boolean subtraction approach is an exact and analytical approach. It directly performs the Boolean subtraction operation between a solid model and the volume swept by a cutter between two adjacent tool positions for simple tools and motions [8-12]. Although this approach can provide accurate verification and error assessment, the computation cost is known to grow too much for a large number of tool-paths [7]. The second approach uses spatial partitioning representation to define a cutter and the workpiece.

In this work, B-rep based method is developed to find the cutter/workpiece engagement (CWE). The most common schemes used in solid modelers are the boundary representation (B-rep) and Constructive Solid Geometry (CSG). In B-rep methodology an object is represented by both its

boundaries defined by faces, edges, vertices and the connectivity information. The prototype program is implemented using the commercial Parasolid solid modeler kernel. Figure 6 and Figure 7 show machined in-process workpieces for different CL locations.
Once the in-process workpiece is obtained for each CL point, the contact patch surface between the tool and workpiece can be extracted by using Parasolid functions. Then, the resulting 3D contact surface, as illustrated in Figure 4 , is projected to the plane perpendicular to the cutter axis by using parasolid functions.
This step finds the enclosing boundaries and curves of the contact patch. Since the force model discretizes the cutter into slices perpendicular to the tool axis and to perform force calculation for each slice, the discs at each level are projected to the plane perpendicular to the cutter axis. The discs are shown by circles in view AA in Figure 4.
Since engagement domain is simply the combination of start and exit angles of each discrete disc located on the cutter, the next step is to assign the start and exit angles to each respective projected disc by intersecting the 2D discs with the boundaries of the contact patch in plane by using Parasolid functions. A final step is required to convert the intersection points into start and exit angles that are required for the force prediction model.
The procedure described above is implemented in Visual Studio.NET using the Parasolid solid modeling Kernel and Parasolid Workshop.

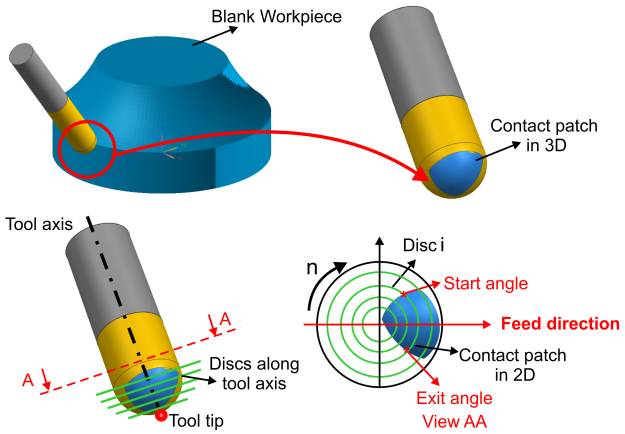

Figure 4: Cutter-workpiece engagement geometry extraction for ball-end mill

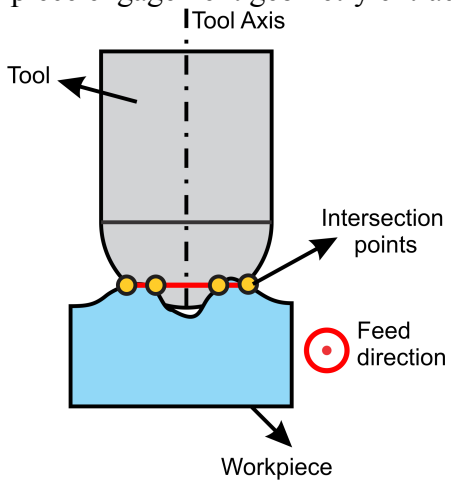

Figure 5: Illustration of multiple contact regions and intersections

The engagement domain results are presented on impeller roughing toolpaths, where the lead and tilt angles change throughout the motion. There are 1572 CL points for this tool path, and the output of the program is processed and the engagement angles are shown together with the contact patches in 2D and 3D for many CL points. Figure 6 shows the engagement for CL points #132 and #1433, where the engagement domain is one piece. However, the engagement domain can have more than one piece because of the complexity of the geometry of the workpiece and the tool motion as shown

simply in Figure 5. In this case, the engagement domain will have more than two intersections (partial engagement regions) for the discs along the cutter. This case was shown for CL points #62 and #164 in Figure 7.

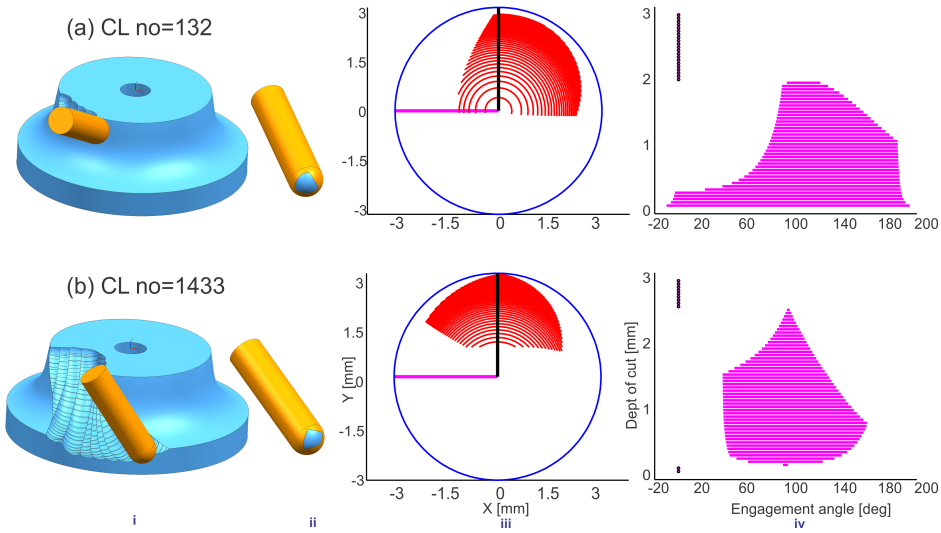

Figure 6: The engagement domain for different CL points

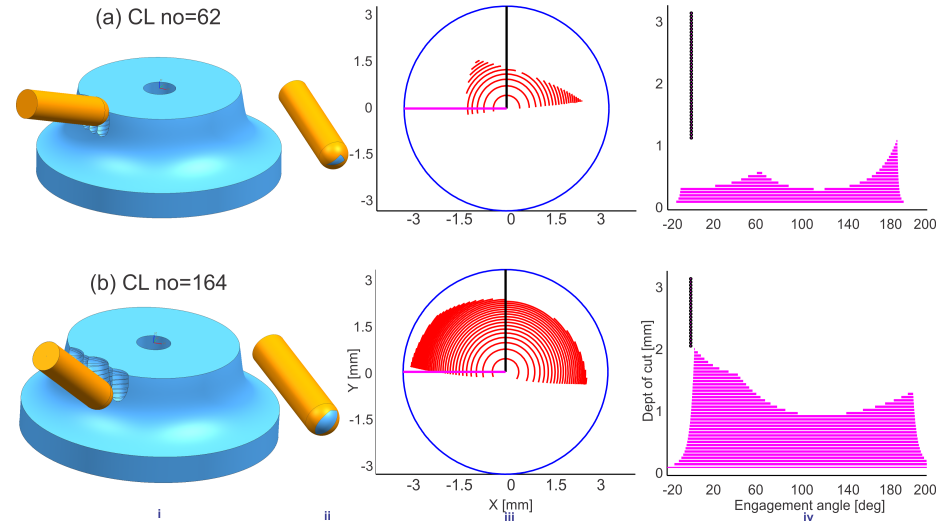

Figure 7: The partial engagement domainsfor different CL points

Cutting Force Model

In milling, cutting forces depend on the instantaneous uncut chip thickness. Hence, for 5-axis machining cutting force predictions, accurate calculation of the chip thickness is quite critical since tool can rotate as well as translate within a toolpath segment.

In free-form surface machining the distance and the rotation angle between two CL points are relatively small, therefore the effect of rotational velocities of the tool is negligible. On the other hand, the effect of the lead and tilt angles on the cut geometry, and horizontal and vertical feed components has to be considered. Distribution of horizontal and vertical chip thickness are shown in Figure 8.

For ball-end mill tool, instantaneous undeformed chip thickness is obtained as follows [10];

$$(t_c)_k = t_x \times \sin(\theta) \times \sin(\psi) \times \cos(\alpha) \pm t_x \times \cos(\psi) \times \sin(\alpha) \quad (5)$$

where $(t_c)_k$ is the chip thickness, t_x is the feed per tooth, θ is the immersion angle of the cutting point, ψ is the cutting element position angle, and α is the feed inclination angle. The immersion angle of a discrete cutting point on the flute of the cutter is given as:

$$\theta = \Omega + 2\pi(n-1)/N_f - \beta_k \tag{6}$$

where θ is the immersion angle for flute n, k represents the number of discrete point on a cutting edge, Ω is the cutting edge rotation angle, N_f is the total number of flutes and β_k is the lag angle due to helix angle of the cutter in the respective kth disk.
The instantaneous infinitesimal chip load is written as follows:

$$dA_c = (t_c)_k \times (dz)_k \tag{7}$$

For a differential chip load dA_c in the engagement domain, the differential cutting forces in radial, axial, and tangential directions (r, ψ, t) is written as follows;

$$\begin{aligned} dF_r &= K_{rc} \times dA_c + K_{re} \times dz \\ dF_\psi &= K_{\psi c} \times dA_c + K_{\psi e} \times dz \\ dF_t &= K_{tc} \times dA_c + K_{te} \times dz \end{aligned} \tag{8}$$

where K_{rc}, $K_{\psi c}$ and K_{tc} are radial, axial and tangential cutting force coefficients and K_{re}, $K_{\psi e}$ and K_{te} are cutting edge coefficients respectively. Cutting force and edge coefficients are determined by mechanistic calibration procedure where these coefficients vary along tool axis direction [10].
Cutting force measurement in 5-axis machining is a challenging task due to the varying orientation of the tool axis with respect to the workpiece. In order to overcome this difficulty a rotating coordinate dynamometer (RCD) is used. RCD is directly attached to the spindle of the machine tool andcutting tool is attached to the dynamometer. In other words, cutting forces are directly measured with respect to tool coordinate frame and the effects of the machine tool rotary axes are eliminated.
Cutting forces in three orthogonal directions ($X_D - Y_D - Z_D$ directions) and the cutting moment about the Z_D axis can be measured with a RCD. $X_D - Y_D - Z_D$ represents the rotating dynamometer coordinate frame.
Consider a two fluted ball-end mill where the cutting flute of the cutter is supposed to be aligned with the X axis of the dynamometer and is traveling along an arbitrary direction. In this position, the angle between Y axis of the dynamometer (Y_D) and the first cutting flute of the cutter is represented as the reference rotation angle Ω_R. The rotation angle Ω is the angle between the cross feed direction and the cutting flute.

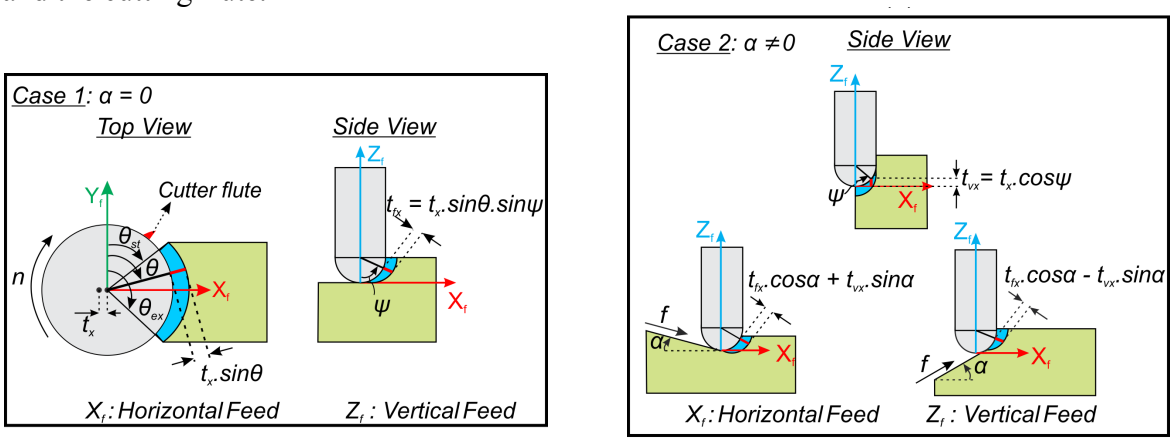

Figure 8: Distribution of chip thickness due to (a) horizontal; (b) vertical feed.

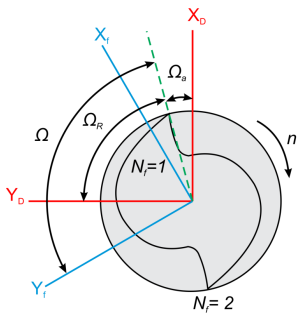

Figure 9: Rotating coordinate frame transformation angles.

Reference rotation angle is constant unless tool alignment changes with respect to dynamometer coordinate frame. In contrary, rotation angle is updated during the simulation at each time step by the given rotation increment angle. For inserted milling cutters and end mills alignment of the cutting flute with the X_D axis can be performed easily, on the other hand, for ball mills due to the complex cutting flute geometry perfect alignment may not be achieved. In this case, a mis alignment angle Ω_a is defined in order to compensate the error introduced. Detailed illustration of the transformation angles is shown in Figure 9.

In order to obtain the transformation from the $(r-\psi-t)$ coordinate frame to feed coordinate frame transformation matrix A is given as,

$$A = \begin{bmatrix} -\sin(\psi)\times\sin(\theta) & -\cos(\psi)\times\sin(\theta) & -\cos(\theta) \\ -\sin(\psi)\times\cos(\theta) & -\cos(\psi)\cos(\theta) & \sin(\theta) \\ \cos(\psi) & -\sin(\psi) & \end{bmatrix} \tag{9}$$

Transformation from the feed coordinate system to rotating dynamometer coordinate frame can be obtained using these matrices,

$$B = \begin{bmatrix} \cos(\Omega_R+\Omega) & -\sin(\Omega_R+\Omega) & 0 \\ \sin(\Omega_R+\Omega) & \cos(\Omega_R+\Omega) & 0 \\ 0 & 0 & 1 \end{bmatrix} \tag{10}$$

$$C = \begin{bmatrix} \cos(\Omega_a) & -\sin(\Omega_a) & 0 \\ \sin(\Omega_a) & \cos(\Omega_a) & 0 \\ 0 & 0 & 1 \end{bmatrix} \tag{11}$$

If the reference rotation angle is known or can be measured, forces in $X_D - Y_D - Z_D$ can be calculated as,

$$\begin{bmatrix} dF_X \\ dF_Y \\ dF_Z \end{bmatrix}_{\text{RCD}} = [B][A]\times\begin{bmatrix} dF_r \\ dF_\psi \\ dF_t \end{bmatrix} \tag{12}$$

If the reference rotation angle is not known or cannot be measured due to complex cutter geometry, misalignment angle can be extracted by running simple slot cutting tests. If this is the case, it is assumed that cutting edge of the cutter is perfectly aligned with the intended coordinate axis of the dynamometer and the misalignment matrix accounts for the misalignment in the calculation.

$$\begin{bmatrix} dF_X \\ dF_Y \\ dF_Z \end{bmatrix}_{\text{RCD}} = [C][B][A]\times\begin{bmatrix} dF_r \\ dF_\psi \\ dF_t \end{bmatrix} \tag{13}$$

Experimental Results and Validation Tests

For the validation of the proposed cutting force modeling approach two different validation tests are presented on impeller roughing toolpaths which are very common in aerospace industry and also constitute typical application for simultaneous 5-axis machining. The simulated toolpath is shown in Figure 10 where lead angles vary between 17° and 66°, and tilt angles vary between 32° and 19°. Dimensions of the blank workpiece and the workpiece coordinate frame are also illustrated in Figure 10.

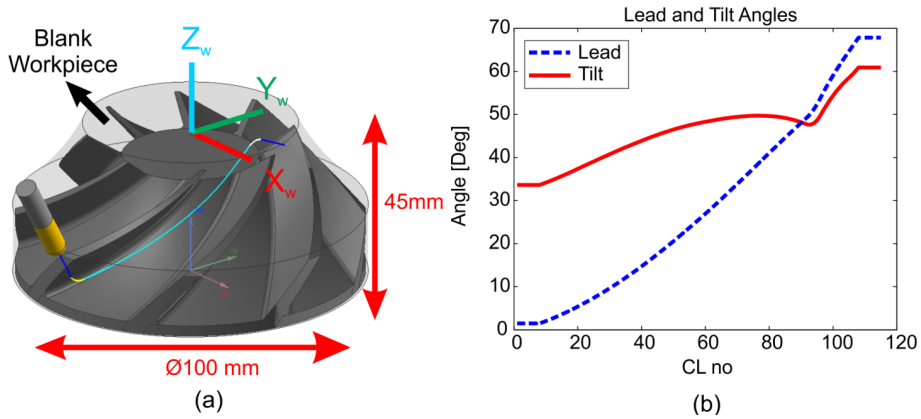

Figure 10: (a) Simulated one-pass impeller roughing toolpath; (b) lead and tilt angles for the toolpath.

In the first test Al7075 workpiece material and a 6 mm diameter carbide cutting are used. Simulated toolpath is generated in NX6 CAM software. In the toolpath, impeller hub surface is used as the drive surface and the orientation of the tool axis is set to the normals of the drive surface (normal to drive). Consequently, a simultaneous 5-axis toolpath is obtained.

Since presented cutting model calculates only static forces chatter-free cutting conditions are identified by utilizing a similar analysis given in [11] . Therefore, spindle speed and the feedrate are selected as 5000 rpm and 250 mm/min respectively. Axial depth of cut varies approximately between 0-1.1 mm. During the cutting operation TCP (Tool center point) control [12] is used in order to keep the relative feedrate between the tool and the workpiece at commanded constant feedrate. For the simulated toolpath, in TCP control mode instantaneous feedrate change approximately between 200 - 1250 mm/min.

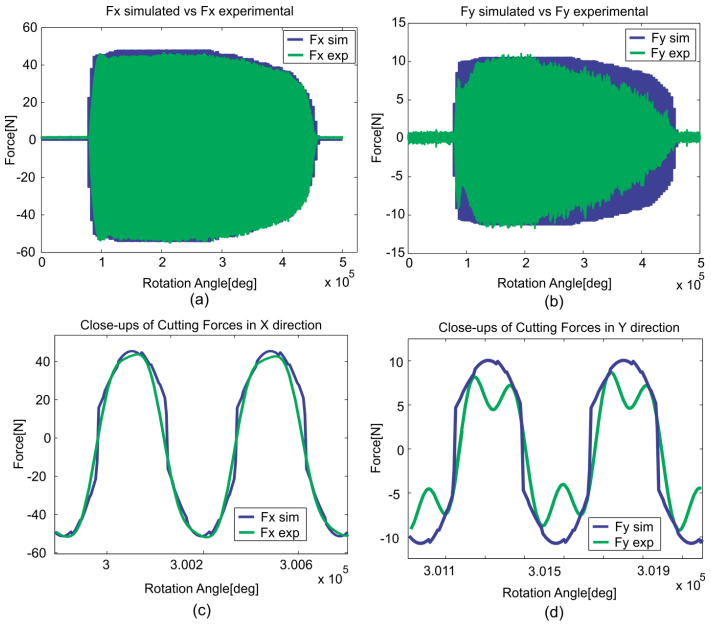

Figure 11: (a) - (b) Predicted versus experimental cutting forces for the entire toolpath; (c)-d) Close-ups of predicted and measured X and Y forces for two revolutions.

Cutting force measurements are performed using Kistler 9123 rotating cutting force dynamometer. The results of the predicted and experimental cutting forces with the close-ups are shown in Figure 11. From the figure, it can be concluded that, predicted cutting forces in X direction match well with the experimental data. In Y direction, there are slight differences in the predicted cutting forces with the experimental data; however the agreement is still reasonably well. The reason for the discrepancy in the Y direction is due to the effect of the measurement noise of the rotary dynamometer which is evident especially at low force magnitudes.

Second validation test is performed for the full roughing toolpath of an impeller hub. Simulated toolpath is generated in NX7.5 CAM software using the Multi Blade Rough method. Generated toolpath consists of 1572 CL points employing zig-zag toolpath with lifts. Axial depth of cut varies approximately between 0-3 mm Details of the toolpath are shown in Figure 12

In the test Al7075 workpiece material and a 6 mm diameter carbide cutting tool are used. Spindle speed and the feedrate are selected as 5000 rpm and 500 mm/min respectively. Cutting tests are performed in TCP control mode and instantaneous feedrate changes approximately between 500 and 6600 mm/min. Forces are collected for every 4 degrees during the machining operation. Output of the simulated machined workpiece and the experimental machined workpiece are shown in Figure 12.

Results of the validation tests are presented in Figure 13 and Figure 14. Figure 13 shows the comparison of the cutting forces for full toolpath and comparison of the cutting force close-ups are illustrated in Figure 14. According to the results, it can be stated that simulated and measured cutting forces match reasonably well within the error band of 0% to 20% although there are minor discrepancy in the predictions.

Trend of the predicted forces are in good agreement with the measured data. Discrepancy of the cutting forces is observed especially in the low axial immersion regions; however this is likely due to low resolution at smaller depth of cuts. Hence, increasing the simulation resolution may increase the simulation accuracy at the cost of computation time.

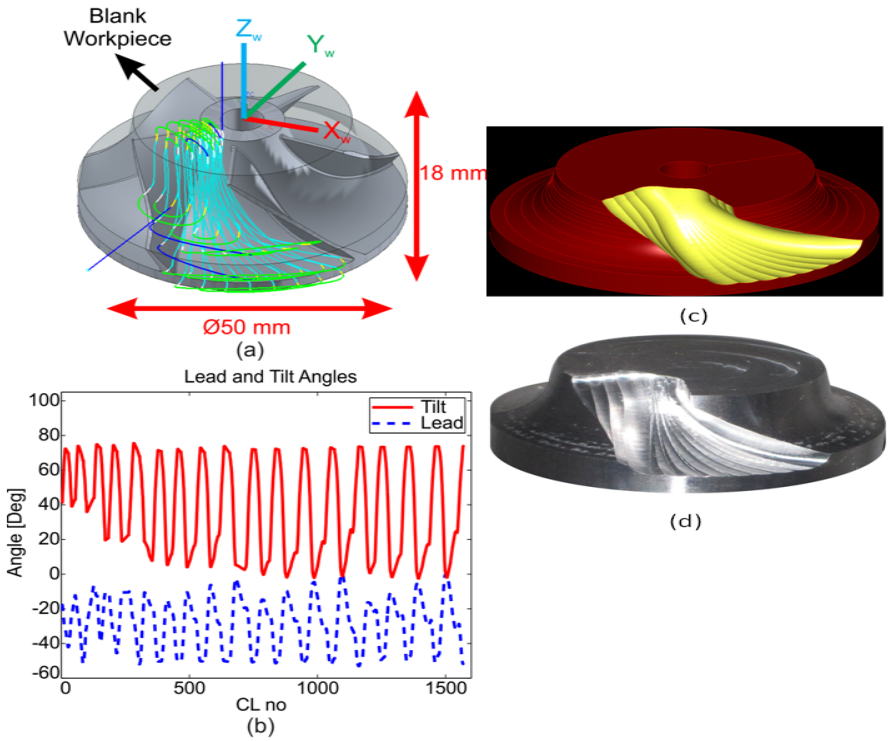

Figure 12: (a) simulated impeller hub roughing toolpath; (b) corresponding lead and tilt angles for the toolpath; (c) simulated part, (d) machined part

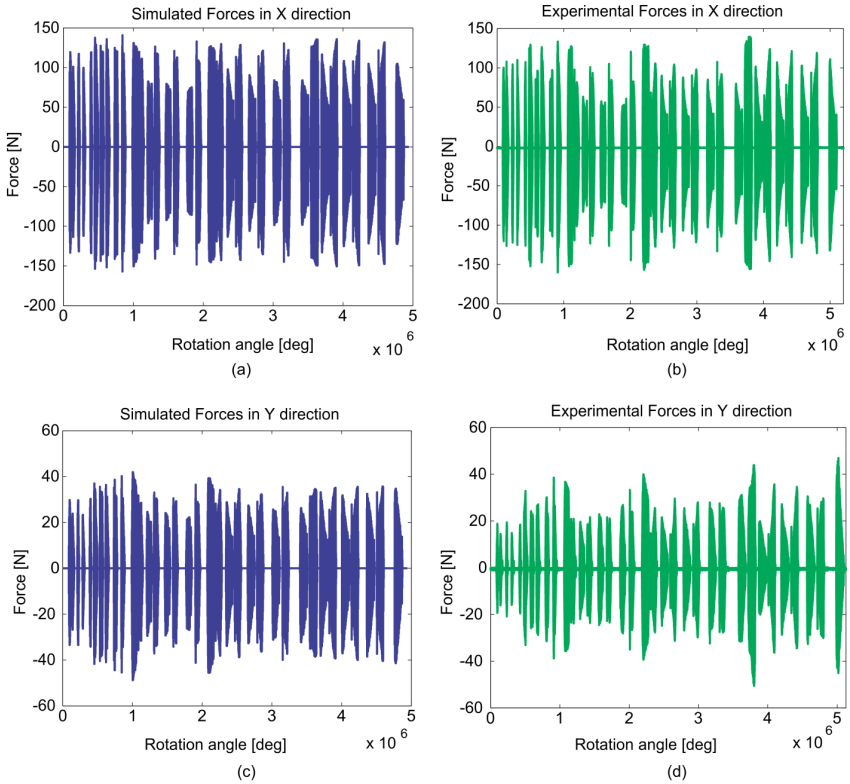

Figure 13: Comparison of predicted and measured cutting forces for the whole toolpath: (a)-(b) X direction; (c) - (d) Y direction

Conclusions

In this paper, a solid-modeler based, boundary representation cutter-workpiece engagement model and a physical model for the prediction of cutting forces in 5-axis ball-end milling process are presented.

In 5-axis ball-end milling, due to variable tool axis orientation, complex workpiece and tool geometry; engagement region between the tool and the workpiece are very complex and irregular. Hence, developed solid-modeler based CWE model provides an efficient and accurate solution by utilizing the exact Boolean approach while extracting the engagement information from the in-process workpiece. Presented cutting force model can predict the 5-axis ball end milling performance accurately via physical modeling of the process. Differential cutting forces for discretized engagement domain are calculated and summed by integrating the differential forces along the engagement angle and axial depth of cut in order to obtain the total cutting force for a toolpath segment.

Validation of the presented approach is demonstrated on different impeller roughing toolpath strategies. Force predictions are shown to be in good agreement with the measured data both in magnitude and trend.

The approach developed based in this model is modular. Therefore, different cutter and workpiece geometries and tool motions can be incorporated into the model without additional analysis. The model has the ability to calculate complex workpiece/cutter intersection domain automatically for a given CL file, cutter and free-form workpiece geometry.

The presented model can be used in industry, for process simulation and process optimization and it can be integrated into CAD/CAM programs. Cutting parameters of an existing 5-axis ball-end milling process can be used in the model to simulate the cutting forces and optimize the feedrate and other cutting parameters in the process.

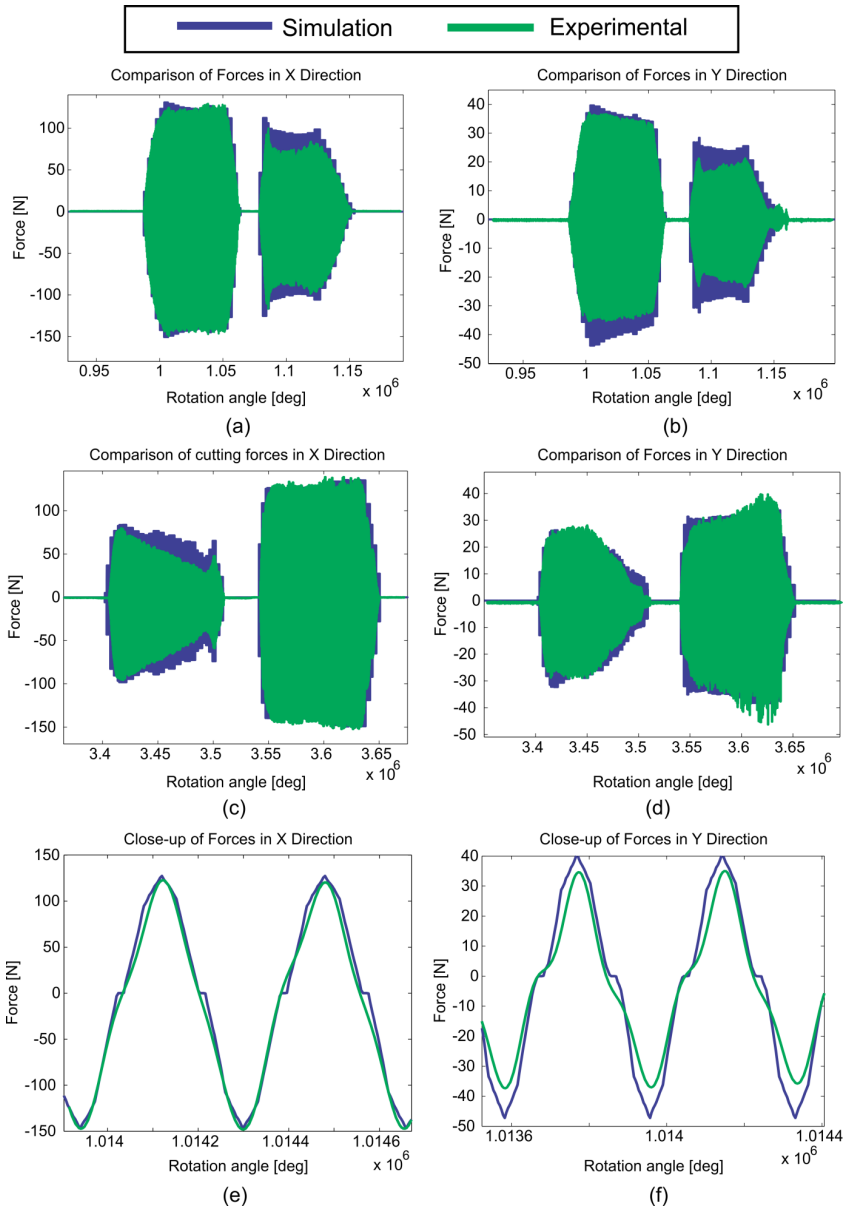

Figure 14: Comparison of cutting force predictions with experiments for two: (a) - (d) tool passes; (e) - (f) tool revolutions

Acknowledgements

The authors greatly appreciate the Machine Tool Technologies Research Foundation (MTTRF), the Mori Seiki Co., the DP Technology Corp, Sanvik Coromant for the Mori Seiki NMV 5000DCG CNC Machining Center, Esprit CAM software and cutting tools to support this research.

References

[1] B.K. Fussell, R.B. Jerard, J.G. Hemmett, Modeling of cutting geometry and forces for 5-axis sculptured surface machining, Computer-Aided Design, 35 (2003) 333-346.

[2] T. Bailey, M.A. Elbestawi, T.I. El-Wardany, P. Fitzpatrick, Generic Simulation Approach for Multi-Axis Machining, Part 1: Modeling Methodology, Journal of Manufacturing Science and Engineering, 124 (2002) 624-633.

[3] E. Ozturk, E. Budak, Modeling of 5-Axis Milling Processes, Machining Science and Technology: An International Journal, 11 (2007) 287-311.

[4] W.B. Ferry, Y. Altintas, Virtual Five-Axis Flank Milling of Jet Engine Impellers—Part I: Mechanics of Five-Axis Flank Milling, Journal of Manufacturing Science & Engineering, 130 (2008) 51-51.

[5] H. Erdim, I. Lazoglu, B. Ozturk, Feedrate scheduling strategies for free-form surfaces, International Journal of Machine Tools and Manufacture, 46 (2006) 747-757.

[6] H. Erdim, I. Lazoglu, M. Kaymakci, Free-Form Surface Machining and Comparing Feedrate Scheduling Strategies Machining Science and Technology: An International Journal, 11 (2007) 117 - 133.

[7] H.B. Voelcker and W.A. Hunt. The role of solid modeling in machining–process modeling and nc verification. In *SAE Tech. Paper 810195*, Warrendale, PA, USA, 1981.

[8] W. Ferry and D. Yip-Hoi. Cutter-workpiece engagement calculations by parallel slicing for fiveaxis flank milling of jet engine impellers. *Journal of Manufacturing Science and Engineering*, 130:051011–12, 2008.

[9] Satyandra K. Gupta, Sunil K. Saini, Brent W. Spranklin, and Zhiyang Yao. Geometric algorithms for computing cutter engagement functions in 2.5d milling operations. *Comput. Aided Des.*, 37(14):1469–1480, 2005.

[10] B. M. Imani, M. H. Sadeghi, and M. A. Elbestawi. An improved process simulation system for ball-end milling of sculptured surfaces. *International Journal of Machine Tools and Manufacture*, 38(9):1089 – 1107, 1998.

[11] Yasumasa Kawashima, Kumiko Itoh, Tomotoshi Ishida, Shiro Nonaka, and Kazuhiko Ejiri. A flexible quantitative method for nc machining verification using a space-division based solid model. *Vis. Comput.*, 7(2-3):149–157, 1991.

[12] A. D. Spence and Y. Altintas. A solid modeller based milling process simulation and planning system. *Journal of Engineering for Industry*, 116:61–69, 1994.